JOURNAL OF MATERIALS SCIENCE 28 (1993) 2887–2892

Superconducting ceramics: preparation, XRD, SEM and EPR measurements to study the influence of compositional variations on superconductivity of La–(Ba/Sr/Ca)–CuO ceramic systems

M. SAKHAWAT HUSSAIN, G. D. KHATTAK*, VEPAN KEITH*, MANSOUR A. AI-SHAFEI
*Chemistry Department, and *Physics Department, King Fahd University of Petroleum and Minerals, KFUPM Box 1830, Dhahran 31261, Saudi Arabia*

A systematic substitution of strontium ions by barium and/or calcium ions in the 21-structure ternary oxide $La_{1.85}Sr_{0.15}CuO_{4-y}$, considered as the host system in this study, was carried out to produce four- and five-component metal oxides of the type $La_{1.85}(Sr_{0.15-x}R_x)CuO_{4-y}$ where R = Ba and/or Ca and $x < 0.15$. A series of samples was prepared using an oxalate co-precipitation procedure where high-purity starting materials, usually required in solid-state pyrolysis reactions, were not required. The experimental conditions for co-precipitation, annealing and pulverization processes were optimized. The X-ray powder diffraction patterns were used to indicate when the materials would become superconducting after annealing. The transition temperatures, T_c, were measured from resistance versus temperature data which confirm that strontium is the best alkaline-earth metal among calcium, barium and strontium. Substitution or partial doping of strontium by calcium and/or barium in the host system decreased the T_c of these ceramics. SEM measurements were carried out to determine the grain size of these materials and characteristic electron paramagnetic resonance spectra for these materials at different temperatures are reported.

1. Introduction

High-temperature superconductivity in 21-structure ternary (and also in quaternary) metal oxides is highly sensitive to compositional variations [1, 2]. The dependence of superconductivity on Sr^{2+} content in ternary $La_{2-x}Sr_xCuO_4$ identified $x = 0.15$ as an optimum concentration with $T_c = 36.5$ K and a transition width (a change in resistance from 10%–90%) of 3 K. Thus, $La_{1.85}Sr_{0.15}CuO_4$ is the optimum stoichiometry for the 21-structure ternary oxide and any deviation from an La:Sr ratio of 1.85:0.15 resulted in a decrease in the T_c of the material [1]. Most of the studies dealing with the compositional variations involved replacement of one or more component in the La–Sr–CuO (or Y–Ba–CuO) systems, by another component of the same type which mostly resulted in a sizable reduction of T_c, though not enough to destroy it [3–6]. Studies dealing with partial doping of rare-earth (RE) or alkaline-earth (AE) component in the known high-T_c material with another AE or RE keeping the overall RE or AE contents the same, have not been reported in the literature.

The ceramic materials, having La:Cu ratio of 1.85:1.00 and strontium-doped with calcium and/or barium to form quaternary oxides such that the total AE metal concentration remains at 0.15, are the subject of this study which has been carried out as a part of our continuing research programme dealing with the preparation and characterization of superconducting and semiconducting materials [7, 8]. A systematic substitution of strontium by barium and/or calcium ions was carried out in $La_{1.85}Sr_{0.15}CuO_4$ to prepare a series of samples using an oxalate co-precipitation procedure. The transition temperature, T_c, was found to be dependent upon sintering and annealing conditions [9]. Thus, the experimental conditions for co-precipitation, annealing, pulverization, effects of oxygen atmosphere, reaction with the porcelain crucible and other experimental manipulations were optimized. The X-ray diffraction (XRD) patterns of the powder, and scanning electron microscopy (SEM) measurements were used for characterization of these materials, while energy dispersive X-ray spectroscopy (EDX) was used for determining the RE:AE ratio in these samples. The resistance versus temperature measurements were carried out on all samples to determine the T_c of these samples. Furthermore, we aimed at (a) optimization of experimental conditions and suitable modifications of the oxalate co-

0022–2461

precipitation method to prepare mixed RE–AE–CuO oxalates using reagent-grade starting materials, (b) optimization of calcination conditions which have strong impact upon powder characteristics such as particle size, morphology, phase composition and microscopic homogeneity, (c) systematic XRD studies showing the effects of compositional variations on the T_c of known superconducting ceramics, and (d) SEM measurements of a few representative samples to investigate their particle size, morphology and microstructures. A consistent set of XRD, SEM and T_c data is not available on the same series of ceramics samples using a similar preparative procedure and we directed our efforts toward obtaining a complete set of data for La–(Sr/Ba/Ca)–CuO_4 series having different AE concentrations.

2. Experimental procedure

2.1 General procedure for preparation of superconducting materials using the oxalate co-precipitation method

All samples reported in this work were prepared by the oxalate co-precipitation method using the following general procedure. Stoichiometric amounts of reagent-grade RE oxides, AE carbonates and CuO were dissolved in 20–30 ml concentrated nitric acid to obtain a clear bluish-green solution. The solution was boiled to almost dryness to remove NO_2 gas and the residue was heated with 10% oxalic acid for complete precipitation of light-blue colour mixed RE, AE and copper oxalates. The oxalate mixture was centrifuged to separate the residue which was dried overnight, with two intermediate grindings, at about 90 °C using an alumina crucible. The residue was then calcined for 28 h at 860 °C with three intermediate grindings to obtain a black homogeneous powder which was further calcined for about 15 h at 900 °C. The powder was hydraulically pressed into pellets (1 cm diameter, 3–4 mm thick) under a pressure of about 20 000 p.s.i. (10^3 p.s.i. = 6.8 N N mm^{-2}). The pellets thus obtained were first sintered for 8–12 h at 800–900 °C, then pulverized into an homogeneous black powder and again sintered for another 8 h at 800–900 °C, compressed again into pellets at 30 000 p.s.i., sintered for 12 h at 900 °C, for 2 h at 1100 °C, for 6 h at 900 °C, and slowly cooled to 450 °C at a cooling rate of 50 °C h^{-1} over a period of 8–10 h, and finally cooled to room temperature. Nine samples of La–(Ba/Sr/Ca)–CuO series with the compositions given in Table I were prepared using the above procedure.

TABLE I Stoichiometries of various samples of La–(Ba/Sr/Ca)–CuO series with different AE contents

Sample	Composition
A	$La_{1.85}Sr_{0.15}CuO_4$
B	$La_{1.60}Sr_{0.40}CuO_4$
C	$La_{1.85}(Sr = Ba = Ca = 0.05)CuO_4$
D	$La_{1.85}Ba_{0.15}CuO_4$
E	$La_{1.85}(Sr = Ba = 0.075)CuO_4$
F	$La_{1.85}(Sr = Ca = 0.075)CuO_4$
G	$La_{1.85}(Ba = Ca = 0.075)CuO_4$
H	$La_{1.85}Ca_{0.15}CuO_4$
I	$La_{1.60}Ca_{0.40}CuO_4$

2.2. X-ray diffraction (XRD) measurements

Each sample for XRD analysis was ground to 200 mesh size and about 1.5 g sample was cemented on top of an aluminium cylinder. The surface of the specimen was pressed, scraped and excess powder was removed to form a flat surface. The XRD patterns were recorded at room temperature using a vertical Q-20 scanning PW-1700 Philips diffractometer. The diffractometer operating conditions were: normal fine-focus sealed-off copper target X-ray tube, $\lambda = 0.0154\,060$ nm, 45 kV, 40 mA, 6.00° take-off angle, 1° divergence slit, 0.2 mm receiving slit, graphite diffracted beam monochromator, rotating specimen, vacuum path, 35%–70% window, and 140° high angular limit. The diffractometer was calibrated using a silicon powder standard. The diffractograms of each of the nine samples were obtained several times at various stages of fabrication to investigate any changes before and after sintering and annealing of each sample. Three diffractograms of representative Samples B, D and E are shown in Figs 1–3.

2.3. SEM and EDX measurements

High-T_c superconductors are polycrystalline materials whose electrical, magnetic and mechanical properties are critically dependent upon their microstructures. In order to investigate the grain size and the microstructure of the specimen, the SEM measurements were carried out on three representative samples, A, D and E, using a Jeol JSM-35CF scanning electron microscope. Electrons from a filament under a pressure of about 10^{-5} torr (1 torr = 133.322 Pa), accelerated by a voltage in the range of ~25 kV, were used. The electron beam was demagnetized in the condenser lens and then focused on to the uncoated sample cemented in the sample holder by silver paste. The scanning electron micrographs were taken at magnifications of X600, X4000 and X10000 and are shown in Fig. 4. The chemical analyses for lanthanum, strontium, barium and copper were done by energy dispersive X-ray microanalysis (EDX) using a Kevex Micro-X7000 on the samples used for SEM measurements. The results of EDX confirmed the following compositions for the three representative samples analysed by EDX after annealing: Sample A = $La_{1.85}Sr_{0.15}CuO_4$, Sample D = $La_{1.85}Ba_{0.15}CuO_4$, and Sample E = $La_{1.85}(Sr = Ba = 0.075)CuO_4$.

2.4. Resistance versus temperature measurements

The collinear four-probe array was used for the measurement of the resistance, R(mohm), of the material versus the temperature, T(K), of the annealed pellets. The samples were of uniform thickness, rectangular-shape, and were sliced with a diamond-impregnated wire saw from the central part of a pellet. The contacts were made using pressed indium. The resistance was

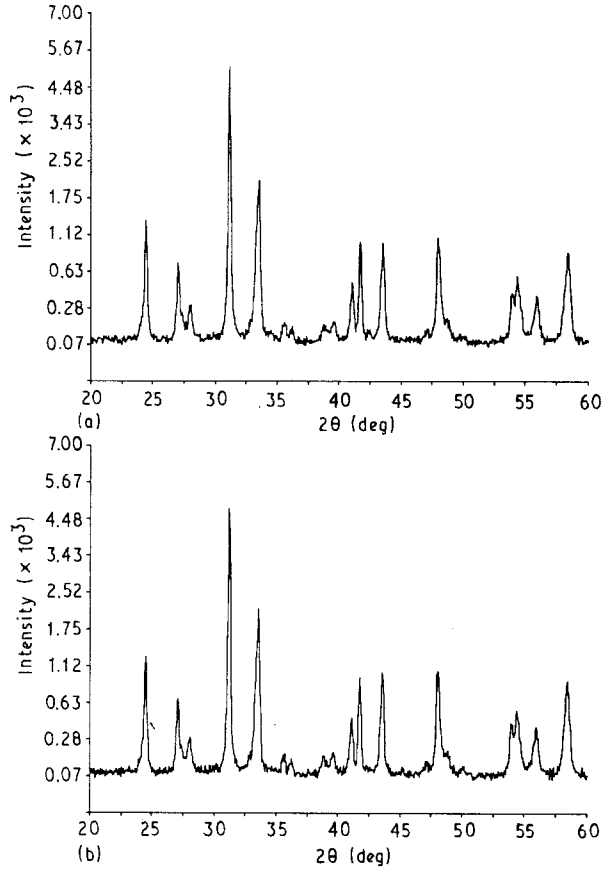

Figure 1 Room-temperature XRD patterns of Sample E ($La_{1.85}$(Sr = Ba = 0.075)CuO_4: (a) before annealing and (b) after annealing, depicting a decrease in the peak intensity ratio (I_1/I_2) from 2.433 to 2.241 for the strongest peaks between 30° and 35°.

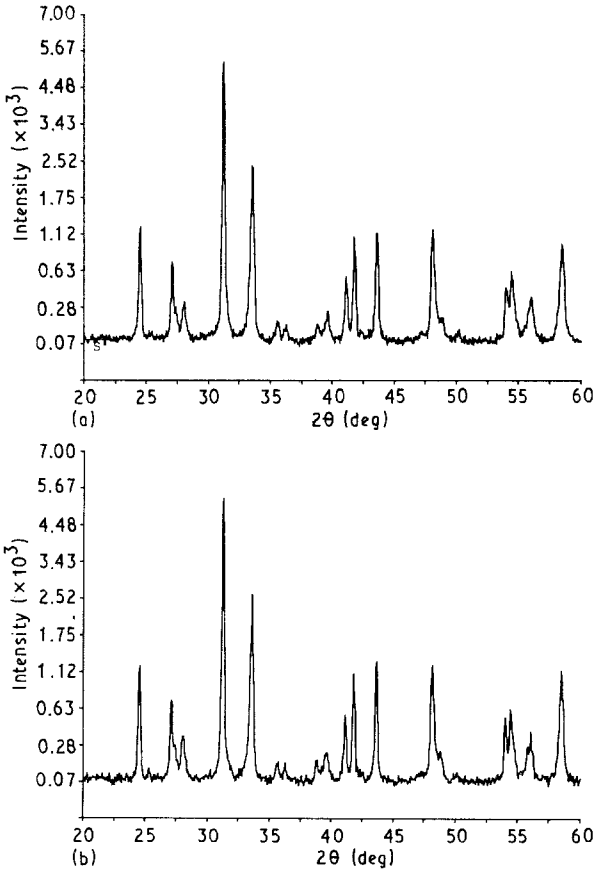

Figure 2 Room-temperature XRD patterns of Sample D ($La_{1.85}Ba_{0.15}CuO_4$: (a) before annealing and (b) after annealing, depicting an increase in the peak intensity ratio (I_1/I_2) from 2.293 to 2.912 for the strongest peaks between 30° and 35°.

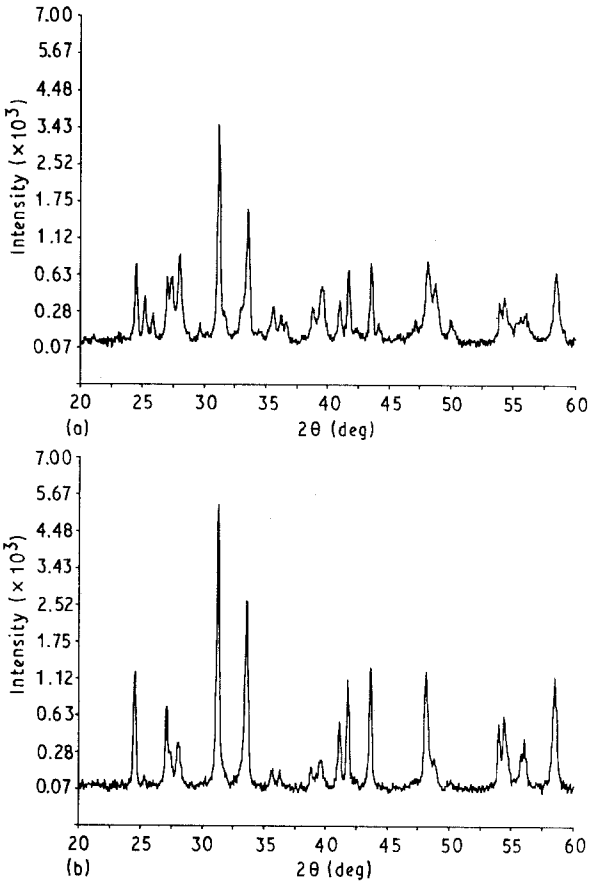

Figure 3 Room-temperature XRD patterns of Sample B ($La_{1.60}Sr_{0.40}CuO_4$: (a) before annealing and (b) after annealing depicting the disappearance of a triple peak and reversal of peaks between 25° and 30°.

measured over the temperature range 4.2 K–100 K. The sample temperatures were determined by a calibrated germanium resistance thermometer embedded in the copper block used for mounting the samples. The data were plotted using KFUPM Data Processing Center facilities. The R–T plots for the whole La–(Ba/Sr/Ca)–CuO series are given in Fig. 5. All curves are indicative of superconducting materials with a clear superconducting transition and the T_c varying with the change in composition.

2.5. Electron paramagnetic resonance (EPR) measurements

EPR measurements were performed with a Varian E-109 spectrometer interfaced with an E-953 data acquisition system at the X-band frequency of 9.1 GHz and a modulation of 100 kHz. Recorded spectra were digitized and stored on cassette tapes. The temperature was controlled by a Varian E-257 variable temperature unit to within + 0.5 °C. The absolute temperature was checked at geometric centre of the cavity with a copper–constantan thermocouple and found to be accurate to + 1 °C. The microwave frequency was measured with a Hewlett–Packard Model 5342 digital frequency counter. The magnetic field sweep was calibrated with a Varian E-500-2 self-tracking nuclear magnetic resonance gaussmeter with an accuracy of + 0.01G. A representative spectrum recorded on a 1 kG sweep is shown in Fig. 6.

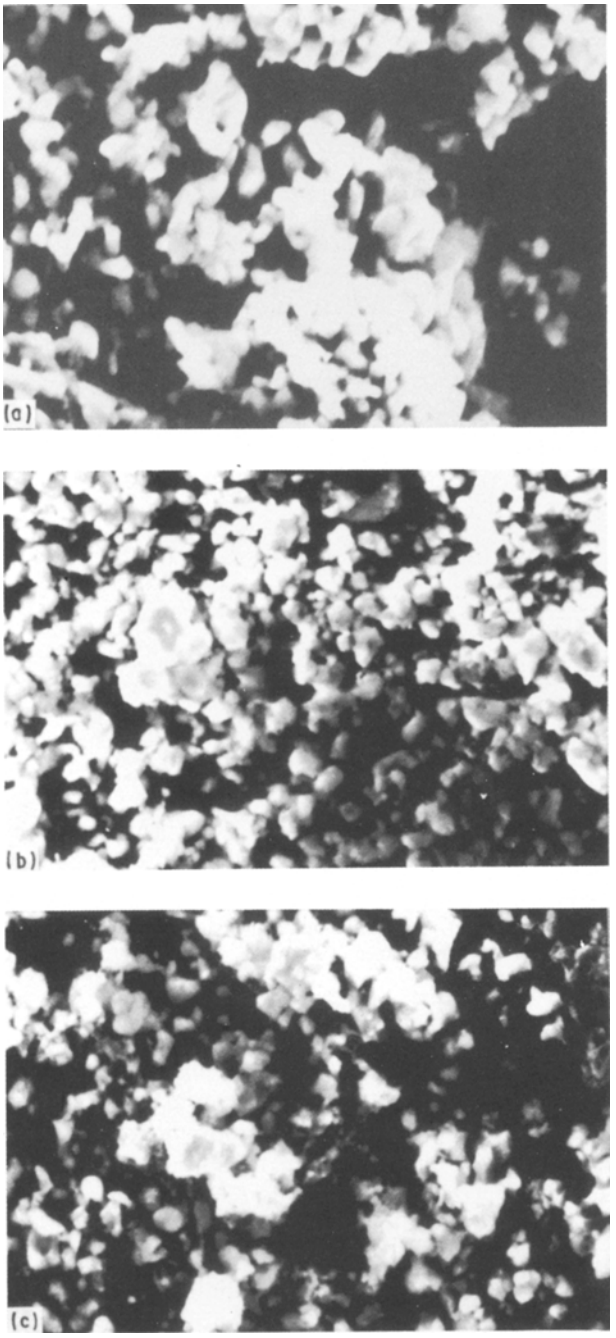

Figure 4 Scanning electron micrographs of three representative samples (a) A, (b) D and (e) E showing the fine microstructure and crystal alignments in the samples X10 000.

3. Results and discussion

3.1. The oxalate co-precipitation method

This method of preparation has the advantage of using the reagent-grade starting materials as compared to high-purity materials needed in the solid-state pyrolysis method. On the basis of the fabrication procedure and the concurrent XRD/SEM measurements carried out during the fabrication of the materials, it could be concluded that the oxalate co-precipitation technique has several additional advantages over the commonly used solid-state pyrolysis method. Some of these advantages are due to the fact that when using the oxalate co-precipitation procedure (a) smaller grain size and better homogeneity are obtained through controlled precipitation of the mixed oxalates from their solution, (b) conversion of oxalates, as compared to carbonates, to oxides is easier, (c) annealing under an oxygen atmosphere was not necessary for the La–(Ba/Sr/Ca)–CuO series, in contrast to the ceramic oxides (Y/Gd)–Ba–CuO having the 123-structure [9], (d) better stoichiometric ratios are obtained through this procedure, and (g) high reproducibility and general applicability over a wide variety of samples was possible. While using oxalate co-precipitation for preparing superconducting material, the following should be carefully observed: (a) a porcelain crucible is not suitable during the firing process, (b) intermediate grinding at least twice during the first 12 h firing and pelletization is necessary, (c) annealing under an oxygen atmosphere and a slow cooling rate are required for (Y/Gd)–Ba–CuO series [9] while oxygen annealing is not necessary for La–(Sr/Ba/Ca)–CuO series.

3.2. XRD patterns for La(Ba/Sr/Ca)–CuO series

The XRD patterns (Figs 1–3) revealed almost identical line positions before and after annealing with the annealed samples having relatively sharper peaks and diminished background absorptions. No general relationship between the peak intensity ratios of the samples, before and after annealing, could be delineated from the strongest XRD peaks appearing in the range 30.0°–35.0°. The peak intensity ratio (I_1/I_2) before and after annealing of Sample E ($La_{1.85}$(Sr = Ba = 0.075)CuO_4) (Fig. 1) decreases while the reverse took place in the case of Sample D ($La_{1.85}Ba_{0.15}CuO_4$) (Fig. 2) where the AE contents were changed from Sr = Ba = 0.075 (Sample E) to only Ba = 0.15 (Sample D). From consideration of the ionic radii [10] (Ba^{2+} = 0.134 nm, and Sr^{2+} = 0.112 nm), one could estimate that the replacement of Ba^{2+}, with larger radius, by Sr^{2+} would affect the CuO_2 layers in the ceramic materials. This should eventually be reflected in the T_c measurement (see below). Annealing the compressed pellet of the black powder for 6–9 h at 900 °C sharpened peaks and reduced the background intensities of all samples in the La(Ba/Sr/Ca)–CuO series (Figs 1–3). When the Sr^{2+} content was increased to 0.40 (Sample B) the peaks at 25.0°–30.0°, which were split into triplets in the unannealed sample, reversed in shape after annealing, which was not the case with the rest of the samples having strontium ions equal to or less than 0.15. There were three peaks in the range 22.0°–27.0° in Sample B before annealing, but after annealing, the intensity of the first peak increased, and the other two peaks disappeared completely. The group of XRD peaks at 37.0°–40.0°, 47.0°–50.0°, and 52.0°–55.0° increased in intensity for all samples after annealing but no shape reversal was observed. The XRD patterns of Samples D, E, F, G and H showed no peak reversal except that the intensities were slightly increased and all minor background absorption peaks completely disappeared after the samples were annealed, which was expected because the sintering mechanism is of practical importance and is the best

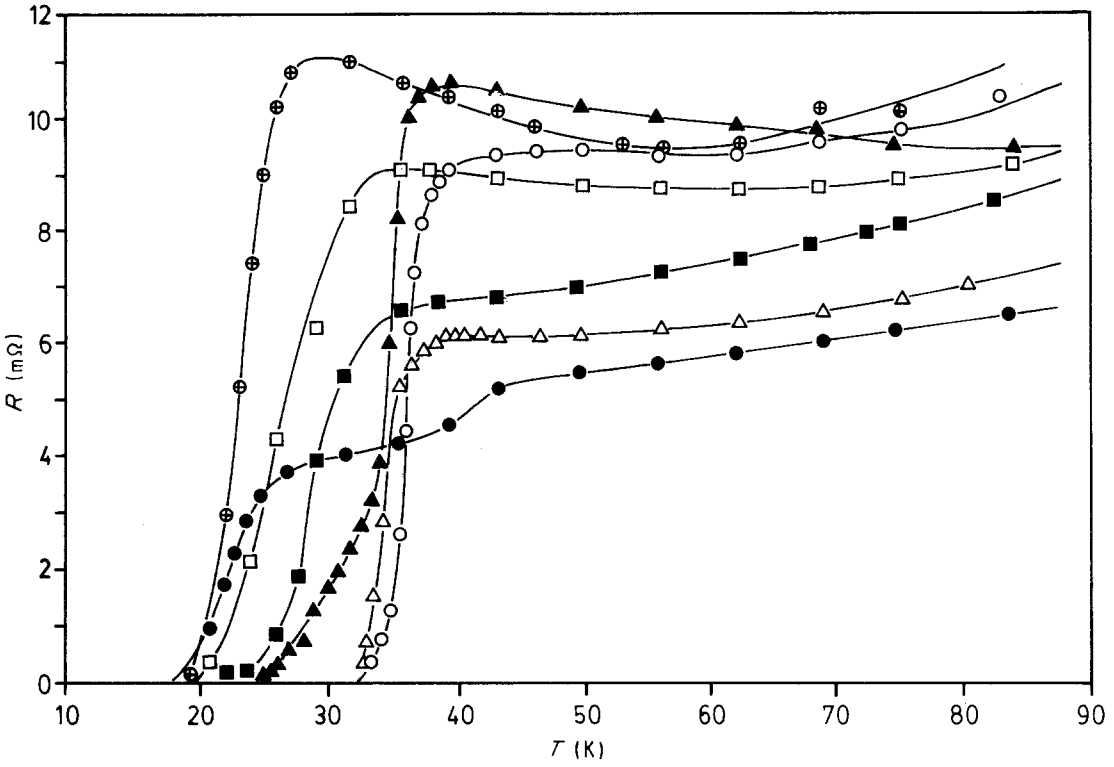

Figure 5 Resistance R (mohm), as a function of temperature, T(K), showing the effects of compositional variations on the T_c of various samples prepared during this study. (○) Sr = 0.15, (●) Sr = 0.40, (□) Sr = Ba = Ca = 0.05), (■) Ba = 0.15, (△) Sr = Ba = 0.075, (▲) Sr = Ca = 0.75, (⊕) Ba = Ca = 0.075.

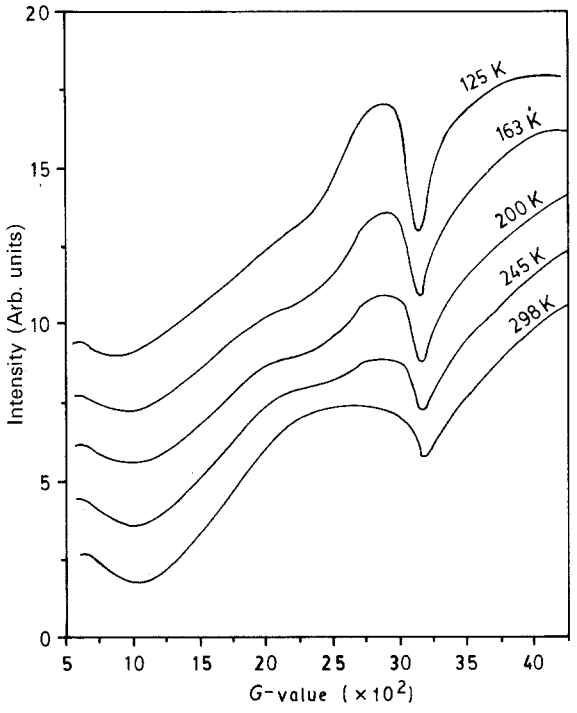

Figure 6 ESR derivative spectra for the host sample as a function of temperature.

way to control the development of microstructure [11].

3.3. SEM and EDX studies

Scanning electron micrographs at X4000 and X10 000 (Fig. 4) revealed that all samples of La–(Sr/Br/Ca)–CuO series were uniformly mixed, which is one of the advantages of the co-precipitation method. Sample D was more condensed, with smaller grain size compared to Samples A and E. Variation in atomic radii affect the grain growth, which takes place during the sintering mechanism. It is clear from scanning electron micrographs and EDX analyses that only one phase was present in all La–(Sr/Ba/Ca)–CuO samples of 21-structure except Sample B. Microstructures have some relationship with the T_c. Although no definitive conclusion can be drawn, our results suggest that as the grain size decreases, the transition temperatures also decrease. The grain size ranges from 0.5–4.85 mm with the smaller grains equiaxed, while the larger are irregular in shape. Sample A shows a grain size of about 4.85 mm (T_c = 36.5 K), while Sample D shows a grain size of 0.86 mm (T_c = 29.5 K). Also, quantitative analyses confirmed the cation ratio of 2:1 for the La:Cu in all samples of the La–(Ba/Sr/Ca)–CuO series.

3.4. Resistance, R(mohm), versus temperature, T(K)

Resistance versus temperature curves for nine samples of the La–(Ba/Sr/Ca)–CuO series are shown in Fig. 5. The resistance was measured over the temperature range 4.2–100 K. The T_c, T_c(onset) and transition width for La(Br/Sr/Ca)CuO_4 are listed in Table II. The T_c(onset) point is defined as the intersection of straight lines extrapolated from the normal-state resistance and the sharp drop in resistance. Transition width is defined as the temperature width corresponding to a change in resistance from 10% to 90% and the mid-point of the transition width is the transition temperature, T_c.

TABLE II Compositional variations and transition temperature data for the La–(Ba/Sr/Ca)–CuO series having 21-structure.

Sample	Composition	T_c(onset) (K)	T_c (K)	Width (K)
A	$La_{1.85}Sr_{0.15}CuO_4$	37	36.5	3
B	$La_{1.60}Sr_{0.40}CuO_4$	25	23.0	6
C	$La_{1.85}$(Sr = Ba = Ca = 0.05)CuO_4	32	26.5	9
D	$La_{1.85}Ba_{0.15}CuO_4$	31	29.5	7
E	$La_{1.85}$(Sr = Ba = 0.075)CuO_4	36	34.5	3
F	$La_{1.85}$(Sr = Ca = 0.075)CuO_4	36	32.0	8
G	$La_{1.85}$(Ba = Ca = 0.075)CuO_4	27	23.0	6
H	$La_{1.85}Ca_{0.15}CuO_4$	26	23.0	6
I	$La_{1.60}Ca_{0.40}CuO_4$	22	17.5	7

All samples exhibited a linear decrease in resistance showing a considerable variation when the concentration of lanthanum and copper was kept constant (equal to that in Sample A) and calcium and/or barium were substituted for strontium such that the total AE contents in the resulting four- or five-component metal oxide systems remained at 0.15. The T_c(onset) was reduced by 10 K from 37 K for Sample A with Sr = 0.15 to 27 K for Sample G with Ca = Ba = 0.075, and the corresponding transition width was broadened by a factor of 2. However, the transition temperature decreased by approximately 10% for up to 50% substitution of barium and/or calcium for strontium (Samples E and F). Further substitution of both barium and calcium for strontium to produce five-component oxide systems with Sr = Ca = Ba = 0.05 (Sample C) resulted in a significant suppression of the T_c as well as T_c(onset) and the transition width increased to 9 K. Total replacement of strontium by calcium or barium (Samples D and H), resulted in the reduction of both T_c and T_c(onset). The transition widths were approximately 6.5 K for La–Ba–CuO or La–Ca–CuO with Ba or Ca = 0.15 and La–Ba/Ca–CuO with Ba = Ca = 0.075, in contrast to 3 K for La–Sr–CuO (Sample A). The T_c for the La–Ba–CuO (Ba = 0.15) was about 6 K higher than for the La–Ca–CuO (Ca = 0.15) and both were lower than that of the La–Sr–CuO (Sr = 0.15) system. An increase in strontium content to 0.4 with concomitant decrease in the lanthanum content from 1.85 to 1.60, resulted in suppression of T_c from 36.5 K to 23.0 K, and complete replacement of strontium by calcium further suppressed T_c to 17.5 K. In addition, Sample B appears to have two mixed phases with an initial T_c(onset) of approximately 43 K.

3.5. EPR measurements

On the assumption that the copper oxide layers in the ceramics are responsible for their superconductivity, the EPR studies were undertaken with the expectation that the Cu^{2+} ion with a $3d^9$ valence configuration should be observable in the EPR of these ceramics. To date, only a few EPR studies on high-T_c superconductors have been reported [12–15] and some authors [15, 16] have reported the absence of any detectable Cu^{2+} signals in these ceramics. EPR of a polycrystalline sample shown in Fig. 6 was recorded at the temperature interval of 80–298 K using liquid nitrogen cooling system. Unlike very weak or absence of EPR signals reported earlier [17] for $YBa_2Cu_3O_7$, quite clear signals but without any fine structure, were observed even at room temperature in the lanthanum-containing ceramics investigated here. The intensity of the broad signals for all samples increased as the temperature was decreased, irrespective of the nature and the amount of the dopant in the parent sample.

Acknowledgements

The authors thank the King Fahd University of Petroleum and Minerals (Chemistry Department and Physics Department) for supporting this research. Thanks are also due to Mr Jamil Bhatti and Mr Martin Sang, ARAMCO, for XRD and SEM measurements.

References

1. R. B. VAN DOVER, R. J. CAVA, B. BATLOGG and E. A. RIETMAN, *Phys. Rev. B* **35** (1987) 5337.
2. A. J. PANSON, A. I. BRAGINSKI, R. J. GAVALER, J. K. HULM, M. A. JANOCKS, H. C. PHOL, A. M. STEWART, J. TALVACCHIO and G. R. WAGNER, *ibid.* **35** (1987) 8774.
3. GANG XIAO, F. H. STREITZ, A. GAVRIN, Y. W. DU and C. L. CHIEN, *ibid.* **35** (1987) 8782.
4. P. H. HOR, R. L. MENG, Y. Q. WANG, L. GAO, Z. J. HUANG, J. BECHTOLD, K. FORSTER and C. W. CHU, *Phys. Rev. Lett.* **58** (1987) 1891.
5. R. J. CAVA, R. B. VAN DOVER, B. BATLOGG and E. A. RIETMAN, *ibid.* **58** (1987) 408.
6. J. G. BEDNORZ, K. A. MULLER and M. TAKASHIGA, *Science* **236** (1987) 73.
7. E. E. KHAWAJA, M. S. HUSSAIN, M. A. KHAN and J. S. HWANG, *J. Mater. Sci.* **21** (1986) 2812.
8. M. S. HUSSAIN, E. E. KHAWAJA and G. D. KHATTAK, *Phys. Status Solidi (a)* **97** (1986) 451.
9. M. S. HUSSAIN, and MANSOUR A. Al-SHAFIE, Proceedings of International Conference on Chemistry in Industry, Bahrain, 14–16 November, 1992, pp. 1223–1225.
10. D. R. CLARK, *Adv. Ceram. Mater.* **2** (3B) (1987) 273.
11. C. P. POOLE Jr, T. DAHA and H. A. FARACH, "Copper Oxide Superconductors", (Wiley Interscience, New York 1988).
12. R. SAEZ PUCHE, M. NORTON and S. W. GLAUNSIGER, *Mater. Res. Bull.* **17** (1982) 1429.
13. K. K. SINGH, P. GANGULY and J. B. GOODENOUGH, *J. Solid State Chem.* **52** (1984) 254.
14. H. THOMANN, R. A. KLEMM, D. C. JOHNSTON, P. J. TINDALL, H. JIN and D. P. GOSHORN, *Phys. Rev. B* **38** (1988) 6552, and references therein.
15. F. MEHRAN, S. E. BARNES, T. R. McGUIRE, W. J. GALLAGHER, R. L. SANDSTROM, T. R. DINGER and D. A. CHANCE, *ibid.* **36** (1987) 740.
16. R. N. SCHWARTZ, *Bull. Amer. Phys. Soc.* **33** (1988) 807.
17. G. J. BOWDEN, P. R. ELLISTON and K. T. WAN, *Austr. Phys.* **24** (1987) 164.

Received 25 July 1991
and accepted 11 March 1992